

Accepted Article

Title: Postsynthetic Functionalization of Three-Dimensional Covalent Organic Framework for Selective Extraction of Lanthanide Ions

Authors: Qianrong Fang, Qiuyu Lu, Yunchao Ma, Hui Li, Xinyu Guan, Yusran Yusran, Ming Xue, Yushan Yan, Shilun Qiu, and Valentin Valtchev

This manuscript has been accepted after peer review and appears as an Accepted Article online prior to editing, proofing, and formal publication of the final Version of Record (VoR). This work is currently citable by using the Digital Object Identifier (DOI) given below. The VoR will be published online in Early View as soon as possible and may be different to this Accepted Article as a result of editing. Readers should obtain the VoR from the journal website shown below when it is published to ensure accuracy of information. The authors are responsible for the content of this Accepted Article.

To be cited as: *Angew. Chem. Int. Ed.* 10.1002/anie.201712246
Angew. Chem. 10.1002/ange.201712246

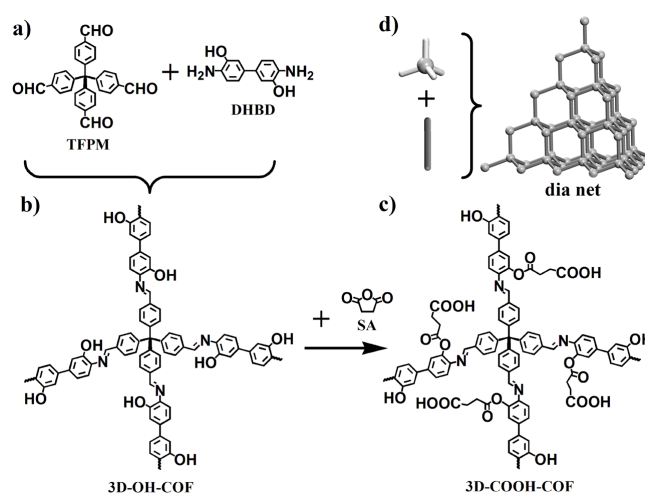
Link to VoR: <http://dx.doi.org/10.1002/anie.201712246>
<http://dx.doi.org/10.1002/ange.201712246>

Postsynthetic Functionalization of Three-Dimensional Covalent Organic Framework for Selective Extraction of Lanthanide Ions

Qiuyu Lu[†], Yunchao Ma[†], Hui Li, Xinyu Guan, Yusran Yusran, Ming Xue, Qianrong Fang*, Yushan Yan, Shilun Qiu and Valentin Valtchev*

Abstract: Chemical Functionalization of covalent organic frameworks (COFs) is critical to tune their properties and broaden their potential applications. However, the introduction of functional groups especially in three-dimensional (3D) COFs still remains largely unexplored. Here we report a general strategy for generating a 3D carboxyl-functionalized COF through postsynthetic modification of a hydroxyl COF, and for the first time explore the 3D carboxyl COF for selective extraction of lanthanide ions. The obtained COF shows high crystallinity, good chemical stability, and large specific surface area. Furthermore, the carboxyl COF displays high metal loading capacities together with excellent adsorption selectivity for Nd³⁺ over Sr²⁺ and Fe³⁺ confirmed by the Langmuir adsorption isotherms and ideal adsorbed solution theory (IAST) calculations. This study not only provides a strategy for versatile functionalization of 3D COFs, but also opens the route to their environmental related applications.

Covalent organic frameworks (COFs) is a new class of crystalline porous polymers based on the precise integration of organic building blocks into periodic structures.^[1] Because of their regular pore structure, high surface area and tunable chemistry, the COF materials are explored in various fields as energy storage,^[2] optoelectronics,^[3] catalysis,^[4] and a number of others.^[5] Over the past decade, a large number of two-dimensional (2D) COFs with nearly eclipsed structures have been synthesized.^[1-5] In contrast, few three-dimensional (3D) COFs have been obtained,^[6,7] and the functionalization of 3D COFs still remains largely unexplored.^[8] Functionalization of the pores of 3D COFs is a straightforward way to predetermine the properties and provide structurally and chemically precise platforms for various applications. However, the introduction of functional groups in 3D COFs is difficult due to the absence of reactive groups, such as hydroxyls, in almost all 3D COFs



Scheme 1. Schematic representation of the strategy for preparing 3D functionalized COF through postsynthetic decoration. (a) Molecular structures of tetra(4-formylphenyl)methane (TFPM) as a tetrahedral building unit and 3,3'-dihydroxybenzidine (DHBD) as a linear linker. (b) 3D COF with hydroxyl groups, 3D-OH-COF, constructed by the condensation reaction of TFPM and DHBD. (c) 3D carboxyl-functionalized COF, 3D-COOH-COF, obtained from the ring opening reaction of 3D-OH-COF with succinic anhydride (SA). (d) A diamondoid (**dia**) net based on tetrahedral and linear building units.

reported to date. Thus, in contrast to zeolites and metal-organic frameworks (MOFs) where the postsynthetic modification is readily used,^[9] the functionalization of 3D COFs is considered to be a great challenge.

Herein, we report a general strategy for preparation of 3D carboxyl-functionalized COF through postsynthetic modification of a hydroxyl COF. The obtained 3D COF shows good crystallinity, high chemical stability, and large specific surface areas. More importantly, the carboxyl COF displays high metal loading capability together with outstanding adsorption selectivity for neodymium(III) over strontium(II) and iron(III) ions as shown by the Langmuir adsorption isotherms and ideal adsorbed solution theory (IAST) calculations. To the best of our knowledge, this study is the first example of the application of 3D COF material for selective extraction of metal ions.

Our strategy for preparation of a carboxyl-functionalized COF, denoted 3D-COOH-COF, is based on the ring opening reaction approach.^[5b] As shown in Scheme 1a, tetra(4-formylphenyl)methane (TFPM) was designed as a tetrahedral building unit, and 3,3'-dihydroxybenzidine (DHBD) was chosen as an ideal linear linker comprising hydroxyl groups. The condensation of TFPM and DHBD produces a 3D hydroxyl COF, 3D-OH-COF (Scheme 1b). Subsequently, the hydroxyl groups in 3D-OH-COF are reacted with succinic anhydride (SA) resulting in a ring opening and formation of

[*] Q. Lu, Y. Ma, H. Li, X. Guan, Y. Yusran, Prof. M. Xue, Prof. Q. Fang, Prof. S. Qiu
State Key Laboratory of Inorganic Synthesis and Preparative Chemistry,
Jilin University, Changchun 130012, China
E-mail: qrfang@jlu.edu.cn
Prof. Y. Yan

Department of Chemical and Biomolecular Engineering,
Center for Catalytic Science and Technology,
University of Delaware, Newark, DE 19716, USA
Prof. V. Valtchev
Normandie Univ, ENSICAEN, UNICAEN, CNRS,
Laboratoire Catalyse et Spectrochimie, 6 Marechal Juin,
14050 Caen, France
E-mail: valentin.valtchev@ensicaen.fr

[†] These authors contributed equally to this work.

Supporting information for this article is available on the WWW under <http://www.angewandte.org> or from the author.

3D-COOH-COF (Scheme 1c). In light of the linking of tetrahedral and linear building units, the structure of both COFs is expected to be based on the diamondoid (**dia**) net (Scheme 1d). Since the tetrahedral TFPM centers are connected by long linear DHBD (10.7 Å), the resulting structure tends to be multi-interpenetrated network.^[10]

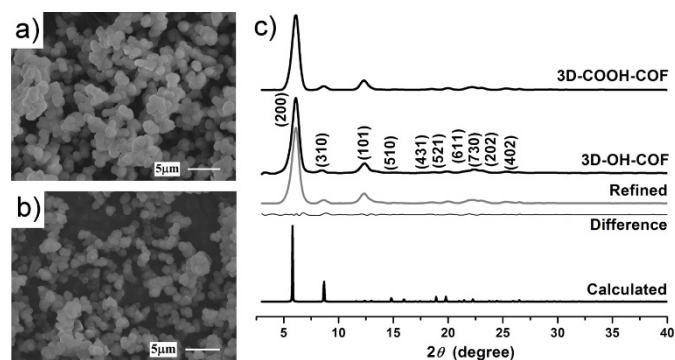


Figure 1. SEM images of 3D-OH-COF (a) and 3D-COOH-COF (b). PXRD patterns (c) of experimentally observed 3D-COOH-COF and 3D-OH-COF, refined 3D-OH-COF, their difference, and calculated 3D-OH-COF based on the 9-fold **dia** net.

The synthesis of 3D-OH-COF was carried out by suspending TFPM and DHBD in the mixed solvent of anhydrous dioxane and mesitylene in the presence of acetic acid followed by heating at 120 °C for 3 days, yielding a crystalline solid. A variety of methods were employed for structural characterizations. The morphology of 3D-OH-COF was examined by scanning electron microscopy (SEM, Figure 1a), which showed isometric crystals with size 1-2 μm. The Fourier transform infrared (FT-IR) spectrum of 3D-OH-COF exhibited a peak at 1626 cm⁻¹ which is characteristic of C=N bond. The concomitant disappearance of the C=O stretching vibration (1693 cm⁻¹) of TFPM and the N-H stretching vibration (3285 and 3354 cm⁻¹) of DHBD, confirmed that a condensation reaction takes place (Figure S1). The solid-state ¹³C cross-polarization magic-angle-spinning (CP/MAS) NMR spectroscopy of 3D-OH-COF confirmed the presence of carbons from the imine groups by the peak at 156 ppm (Figure S2). It is worth noting that the high thermal stability (450 °C) displayed by 3D-OH-COF, as shown by the thermogravimetric analysis (TGA, Figure S3).

The crystalline nature of 3D-OH-COF was revealed by powder X-ray diffraction (PXRD) analysis. PXRD peaks at 5.85, 8.70, 12.41, 14.82, 18.94, 19.81, 21.45, 22.25, 24.45 and 26.52° 2θ can be assigned to the (200), (310), (101), (510), (431), (521), (611), (730), (202) and (402) Bragg peaks (Figure 1c, black curve). The Pawley refinement yielded a PXRD that is in good agreement with the experimentally observed pattern, as evident by their negligible difference and very low values of $wR_p = 3.48\%$ and $R_p = 7.41\%$ (Figure 1c, red and green curves). Considering that the length of these linkers is similar to those of COF-320,^[11] a 9-fold **dia** net for 3D-OH-COF was constructed from TFPM and DHBD by using the Materials Studio Software package (Table S1).^[12] Simulated PXRD pattern shows good match with the experimental one (Figure 1c, pink curve). On the basis of these results, 3D-OH-COF was proposed to have the expected architecture with a 9-fold **dia** net, which shows the microporous rectangular pores with the largest diameter of about 13.5 Å (Figure 2a). The BET surface area was determined to be 1077 m² g⁻¹ from N₂ sorption isotherms at 77 K (Figure 3a, and Figure S4).

DFT fitting of the adsorption branches showed pore size distributions mainly at 13.1 Å in agreement with that of the proposed model (Figure 3a inset).

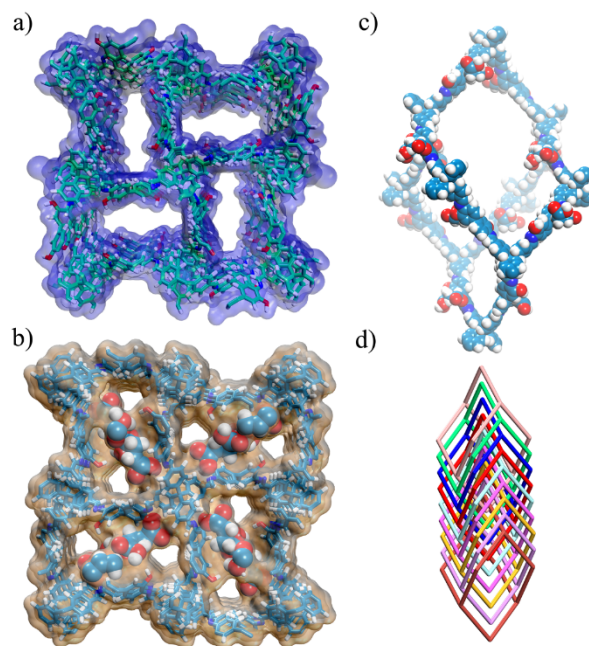


Figure 2. Extended structures of 3D-OH-COF (a) and 3D-COOH-COF (b). Single **dia** network (c) and 9-fold interpenetrated **dia** topology (d) in 3D-COOH-COF.

Inspired by its high crystallinity and abundant presence of hydroxyls, we converted the 3D-OH-COF into a carboxyl-functionalized 3D-COOH-COF based on the ring opening reaction. Typically, 3D-COOH-COF was obtained by suspending 3D-OH-COF in SA (8.0 mL, 1.0 M solution in anhydrous acetone) at 60 °C for 24 h. 3D-COOH-COF and 3D-OH-COF exhibit similar PXRD pattern and morphology, indicating that no noticeable morphological and structural changes occurred during chemical modification (Figure 1b and 1c). Nitrogen sorption measurement revealed substantially reduced BET surface area (540 m² g⁻¹) and pore size (6.8 Å) of carboxyl grafted 3D-COOH-COF (Figure 3b and Figure S5). On the other hand the 3D-COOH-COF shows thermal stability (450 °C) similar with the parent material (Figure S6). The successful grafting of carboxyl groups onto the 3D-OH-COF was confirmed by FT-IR, solid-state ¹³C NMR studies, liquid ¹H NMR spectroscopy of hydrolyzed samples and elemental analysis. The FT-IR spectrum of the 3D-COOH-COF showed the characteristic band of -COOH at 3649 cm⁻¹, confirming the existence of free-standing carboxyl groups (Figure S7). The carboxyl-functionalized transformation was determined by the concomitant emergence of peak at 164.2 ppm ascribed to the carboxyl groups in the ¹³C MAS NMR spectrum of 3D-COOH-COF (Figure S8). Furthermore, elemental analysis and liquid ¹H NMR spectroscopy of hydrolyzed 3D-COOH-COF sample revealed that 50% of available hydroxyls were grafted/replaced with carboxylic groups. This result is attributed to the steric limitations in micropore space (Table S2). The set of experimental data shows that carboxylic groups were successfully incorporated without significantly altering the crystalline structure of 3D-OH-COF (Figure 2 and Table S3). The framework of 3D-COOH-COF was stable in ambient air and retained its crystallinity after soaking in a variety of

organic solvents and water, as well as in acid (3.0 M HCl) and base (3.0 M NaOH) aqueous solutions (Figures S9-12).

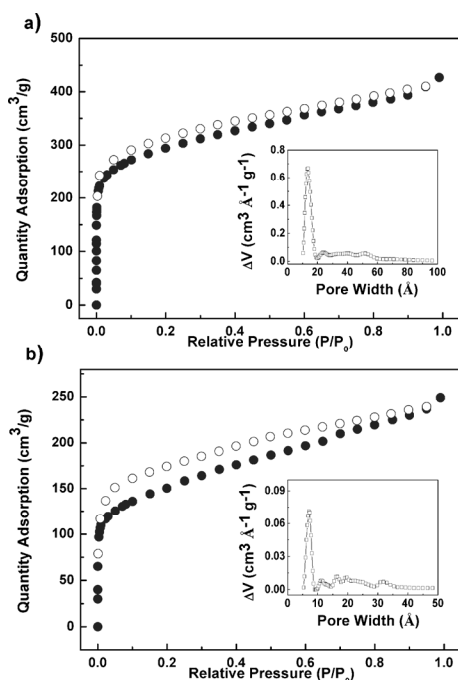


Figure 3. N_2 adsorption-desorption isotherms for 3D-OH-COF (a) and 3D-COOH-COF (b) at 77 K. Solid and open circles represent adsorption and desorption branches, respectively. Inset: pore-size distribution calculated by fitting on the NLDFT model to the adsorption data.

After confirming the porosity, stability, and high density of carboxyl groups available for metal chelating sites, we examined the ability of 3D-COOH-COF to effectively extract lanthanide ions from aqueous solution, as urgent required in the treatment of radioactive waste.^[13] As an initial investigation, the Nd^{3+} , Sr^{2+} and Fe^{3+} ions were chosen as representative ions for group separation of lanthanide fission products, other fission products, and the corrosion products in nuclear waste streams, respectively.^[14] Typically, the uptakes of metal ions by 3D-COOH-COF were measured at room temperature, and the concentrations of metal ions were monitored by using UV-Vis spectrometer. After the reactions, the SEM and PXRD inspection confirmed the structural integrity of 3D-COOH-COF, thus revealing its high stability (Figures S13 and S14).

The extraction capability of 3D-COOH-COF was studied by the adsorption isotherms for metal ion uptakes (Figure 4a). To estimate selectivity, the data were fitted with Langmuir equation, $n = n_{sat}bC/(1 + bC)$, where n is the total amount adsorbed, C is the concentration, n_{sat} is the saturation capacity, and b is the Langmuir parameter that represents the affinity of metal ions for the binding sites. As shown in Table 1, the b parameter for Nd^{3+} (15.87 mM^{-1}) is much higher than those of Sr^{2+} (0.85 mM^{-1}) and Fe^{3+} (0.08 mM^{-1}) ions, which suggests that adsorption of Nd^{3+} is stronger than Sr^{2+} and Fe^{3+} adsorption in 3D-COOH-COF. Indeed, this is highlighted by the steep adsorption isotherm at low concentration. The near vertical rise of the Nd^{3+} adsorption isotherm indicates that Nd^{3+} binds the framework most strongly, followed by Sr^{2+} and Fe^{3+} . These results can be ascribed to the greater charge density of Nd^{3+} relative to Sr^{2+} and the larger ionic radius relative to Fe^{3+} , which provides a better match for certain rigid

binding pockets within 3D-COOH-COF involving multiple carboxyl groups. While Nd^{3+} has the highest uptake at low concentration, Fe^{3+} has the highest uptake at saturation owing to its smaller size, which is consistent with the n_{sat} parameters (0.71 mmol/g for Nd^{3+} , 0.72 mmol/g for Sr^{2+} and 4.86 mmol/g for Fe^{3+}). 3D-OH-COF was used as a reference to extract the above metal ions; however, it shows very low uptakes which can be attributed to the absence of strong exchange sites and thus low extraction power (Figure S15).

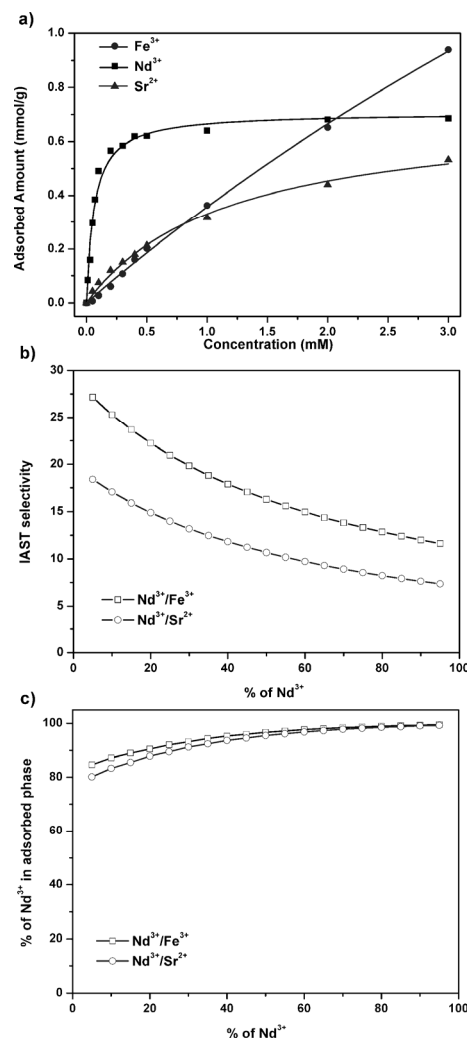


Figure 4. Metal ion adsorption isotherms (a) of 3D-COOH-COF at room temperature. IAST selectivity (b) and purities (c) of 3D-COOH-COF for Nd^{3+}/Fe^{3+} and Nd^{3+}/Sr^{2+} mixtures.

The IAST method has been well established for evaluation of metal ion uptakes by variety of adsorbents.^[15] Consequently we employed this method to predict the mixture behavior of 3D-COOH-COF. Since the relative concentrations of Nd^{3+} , Fe^{3+} and Sr^{2+} ions can fluctuate in a radioactive waste stream, IAST selectivity was calculated over a wide range of compositions for a total concentration of 0.1 mM. As shown in Figure 4b, 3D-COOH-COF exhibits a high selectivity for Nd^{3+} over Sr^{2+} and Fe^{3+} . For instance, for a solution containing 5% Nd^{3+} and 95% Fe^{3+} or Sr^{2+} , 3D-COOH-COF selectively adsorbs Nd^{3+} with an IAST selectivity of 27 and 18, respectively. IAST purity predictions presented in Figure 4c illustrate the effectiveness of metal ion selectivity in 3D-COOH-COF. They show that Nd^{3+} can be isolated from Sr^{2+} and Fe^{3+} solutions at a high

purity, reaching 86% over Fe^{3+} and 80% over Sr^{2+} at a composition of only 5% Nd^{3+} in their mixtures. This suggests that the coordination environment and strength of the metal ion–framework interactions are very uniform in 3D-COOH-COF, and preferential binding is consistent across all sites.

Table 1. Langmuir fit parameters for single-component adsorption isotherms

	Nd^{3+}	Sr^{2+}	Fe^{3+}
b (mM⁻¹)	15.87	0.85	0.08
n (mmol/g)	0.71	0.72	4.86

To gain further insights into the structure–performance relationship of 3D-COOH-COF in the selective detection and effective removal of Nd^{3+} , we applied solid-state ^{13}C NMR spectroscopy to evaluate the interaction between Nd^{3+} and carboxyl groups (Figure S16). After adsorption of Nd^{3+} , the ^{13}C NMR signal at 164.2 ppm, which is ascribed to the carbons of the carboxyl groups in the 3D-COOH-COF, is downfield shifted to 167.1 ppm, while other signals remain unchanged. This result points out the strong interaction between Nd^{3+} and the carboxyl groups in Nd/3D-COOH-COF. As a control, the obtained Sr/3D-COOH-COF and Fe/3D-COOH-COF gave almost identical ^{13}C CP/MAS NMR spectra as 3D-COOH-COF, indicating that no distinct interaction existed between Sr^{2+} (or Fe^{3+}) and 3D-COOH-COF. Moreover, X-ray photoelectron spectroscopy (XPS) provides further evidence for the strong interaction between Nd^{3+} and the carboxyl groups. Compared with the binding energy (BE, 983.7 eV) of Nd 3d_{5/2} in Nd(NO₃)₃, the BE of Nd/3D-COOH-COF was shifted to 980.1 eV (Figure S17). The negative shift by 3.6 eV evidenced the interaction between Nd^{3+} and the carboxyl groups in Nd/3D-COOH-COF: electrons were further donated to Nd^{3+} , which makes the Nd an electron-excess atom.^[16] We further explored the recycle use of 3D-COOH-COF; the Nd^{3+} adsorption–desorption cycle could be repeated at least three times with almost no loss of activity (Figures S18 and S19).

In summary, we report a strategy for functionalizing 3D COFs through postsynthetic modification. The carboxyl-functionalized 3D-COOH-COF showed exceptional lanthanide selectivity (Nd^{3+}) based on the Langmuir adsorption isotherms and IAST calculations. XPS and solid-state NMR investigations verified the strong and selective interaction between Nd^{3+} ions and carboxyl groups in 3D-COOH-COF. Recyclability experiments demonstrated that multiple adsorption/stripping cycles could be performed with minimal degradation of the adsorption capacity of 3D-COOH-COF. This study not only develops a general method for a facile and efficient functionalization of 3D COFs, but also promotes functionalized COF materials into an excellent scaffold for environmental related applications.

Experimental Section

Synthesis of 3D-OH-COF. A Pyrex tube measuring o.d. × i.d. = 10 × 8 mm² was charged with TFPM (21.6 mg, 0.05 mmol) and DHBD (21.6 mg, 0.1 mmol) in a mixed solution of dioxane (0.9 mL), mesitylene (0.1 mL) and acetic acid (0.1 mL, 3 M). The tube was flash frozen at 77 K (LN₂ bath), evacuated to an internal pressure of 0.15 mmHg and flame sealed. Upon sealing the length of the tube was reduced to ca.

13 cm. The reaction mixture was heated at 120 °C for 3 days to afford a white precipitate which was isolated by filtration over a medium glass frit and washed with anhydrous tetrahydrofuran (THF, 20.0 mL). The product was immersed in anhydrous THF (20.0 mL) for 8 h, after that the activation solvent was decanted and freshly replenished four times. The solvent was removed under vacuum at 80 °C to afford the corresponding product as white powder in isolated yield of 81% for 3D-OH-COF.

Postsynthetic functionalization. 3D-OH-COF (46.8 mg, 0.1 mmol) was weighed into a 10-mL glass vial, to which SA (8.0 mL, 1.0 M solution in anhydrous acetone) was added. The reaction mixture was shaken at 60 °C for 24 h. The precipitate was collected by centrifugation, and three times washed with anhydrous THF. The crude product was rinsed with THF for 24 h using a Soxhlet extractor. The powder was dried at 80 °C under vacuum overnight to give the 3D-COOH-COF in yield of 83%.

Further detailed experimental procedures and characterization are described in the Supporting Information.

Acknowledgments

This work was supported by National Natural Science Foundation of China (21571079, 21621001, 21261130584, 21390394, 21571076, and 21571078), “111” project (B07016 and B17020), Guangdong and Zhuhai Science and Technology Department Project (2013B090200052 and 2012D0501990028), Ministry of Education, Science and Technology Development Center Project (20120061130012), and the program for JLU Science and Technology Innovative Research Team. V.V. and Q.F. acknowledge the Thousand Talents program (China). V.V., Q.F. and S.Q. acknowledge the collaboration in the framework of China-French joint laboratory “Zeolites”.

Received: ((will be filled in by the editorial staff))

Published online on ((will be filled in by the editorial staff))

Keywords: covalent organic frameworks · postsynthetic functionalization · porous materials · separation · selective adsorption

- [1] a) A. P. Côté, A. I. Benin, N. W. Ockwig, M. O’Keeffe, A. J. Matzger, O. M. Yaghi, *Science* **2005**, *310*, 1166–1170; b) X. Feng, X. S. Ding, D. L. Jiang, *Chem. Soc. Rev.* **2012**, *41*, 6010–6022; c) S. Y. Ding, W. Wang, *Chem. Soc. Rev.* **2013**, *42*, 548–568; d) J. W. Colson, W. R. Dichtel, *Nat. Chem.* **2013**, *5*, 453–465; e) P. J. Waller, F. Gándara, O. M. Yaghi, *Acc. Chem. Res.* **2015**, *48*, 3053–3063; f) N. Huang, P. Wang, D. L. Jiang, *Nat. Rev. Mater.* **2016**, *1*, 16068; g) C. S. Diercks, O. M. Yaghi, *Science* **2017**, *355*, 923.
- [2] a) P. Kuhn, M. Antonietti, A. Thomas, *Angew. Chem.* **2008**, *120*, 3499–3502; *Angew. Chem., Int. Ed.* **2008**, *47*, 3450–3453; b) W. Tilford, S. J. Mugavero III, P. J. Pellechia, J. J. Lavigne, *Adv. Mat.* **2008**, *20*, 2741–2746; c) S. S. Han, H. Furukawa, O. M. Yaghi, W. A. Goddard III, *J. Am. Chem. Soc.* **2008**, *130*, 11580–11581; d) H. Furukawa, O. M. Yaghi, *J. Am. Chem. Soc.* **2009**, *131*, 8875–8883; e) M. G. Rabbani, A. K. Sekizkardes, Z. Kahveci, T. E. Reich, R. Ding, H. M. El-Kaderi, *Chem. Eur. J.* **2013**, *19*, 3324–3328; f) S. Wang, Q. Wang, P. Shao, Y. Han, X. Gao, L. Ma, S. Yuan, X. Ma, J. Zhou, X. Feng, B. Wang, *J. Am. Chem. Soc.* **2017**, *139*, 4258–4261.

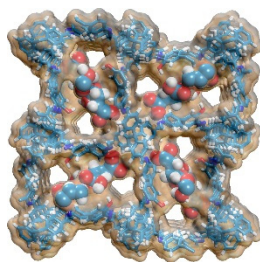
- [3] a) S. Wan, J. Guo, J. Kim, H. Ihee, D. Jiang, *Angew. Chem.* **2008**, *120*, 8958-8962; *Angew. Chem., Int. Ed.* **2008**, *47*, 8826-8830; b) S. Wan, J. Guo, J. Kim, H. Ihee, D. Jiang, *Angew. Chem.* **2009**, *121*, 5547-5550; *Angew. Chem., Int. Ed.* **2009**, *48*, 5439-5442; c) E. L. Spitzer, W. R. Dichtel, *Nat. Chem.* **2010**, *2*, 672-677; d) X. Ding, J. Guo, X. Feng, Y. Honsho, J. Guo, S. Seki, P. Maitarad, A. Saeki, S. Nagase, D. Jiang, *Angew. Chem.* **2011**, *123*, 1325-1329; *Angew. Chem., Int. Ed.* **2011**, *50*, 1289-1293; e) E. L. Spitzer, B. T. Koo, J. L. Novotney, J. W. Colson, F. J. Uribe-Romo, G. D. Gutierrez, P. Clancy, W. R. Dichtel, *J. Am. Chem. Soc.* **2011**, *133*, 19416-19421; f) X. Feng, L. Chen, Y. Honsho, O. Saengsawang, L. Liu, L. Wang, A. Saeki, S. Irle, S. Seki, Y. Dong, D. L. Jiang, *Adv. Mat.* **2012**, *24*, 3026-3031; g) M. Dogru, M. Handloser, F. Auras, T. Kunz, D. Medina, A. Hartschuh, P. Knochel, T. Bein, *Angew. Chem.* **2013**, *125*, 2992-2996; *Angew. Chem., Int. Ed.* **2013**, *52*, 2920-2924; h) G. H. V. Bertrand, V. K. Michaelis, T. C. Ong, R. G. Griffin, M. Dinca, *Proc. Natl. Acad. Sci. USA* **2013**, *110*, 4923-4928; i) M. Calik, F. Auras, L. M. Salonen, K. Bader, I. Grill, M. Handloser, D. Medina, M. Dogru, F. Löbermann, D. Trauner, A. Hartschuh, T. Bein, *J. Am. Chem. Soc.* **2014**, *136*, 17802-17807; j) Y. Du, H. Yang, J. M. Whiteley, S. Wan, Y. Jin, S. H. Lee, W. Zhang, *Angew. Chem.* **2016**, *128*, 1769-1773; *Angew. Chem., Int. Ed.* **2016**, *55*, 1737-1741.
- [4] a) S. Y. Ding, J. Gao, Q. Wang, Y. Zhang, W. G. Song, C. Y. Su, W. Wang, *J. Am. Chem. Soc.* **2011**, *133*, 19816-19822; b) S. Lin, C. S. Diercks, Y. B. Zhang, N. Kornienko, E. M. Nichols, Y. Zhao, A. R. Paris, D. Kim, P. Yang, O. M. Yaghi, C. J. Chang, *Science* **2015**, *349*, 1208-1213; c) V. S. Vyas, F. Haase, L. Stegbauer, G. Savasci, F. Podjaski, C. Ochsenfeld, B. V. Lotsch, *Nat. Commun.* **2015**, *6*, 8508; d) Y. Peng, Z. Hu, Y. Gao, D. Yuan, Z. Kang, Y. Qian, N. Yan, D. Zhao, *ChemSusChem* **2015**, *8*, 3208-3212; e) Q. Sun, B. Aguila, J. Perman, N. Nguyen, S. Q. Ma, *J. Am. Chem. Soc.* **2016**, *138*, 15790-15796; f) X. Wang, X. Han, J. Zhang, X. Wu, Y. Liu, Y. Cui, *J. Am. Chem. Soc.* **2016**, *138*, 12332-12335; g) H. S. Xu, S. Y. Ding, W. K. An, H. Wu, W. Wang, *J. Am. Chem. Soc.* **2016**, *138*, 11489-11492; h) X. Han, Q. C. Xia, J. J. Huang, Y. Liu, C. X. Tan, Y. Cui, *J. Am. Chem. Soc.* **2017**, *139*, 8693-8697.
- [5] a) C. J. Doonan, D. J. Tranchemontagne, T. G. Glover, J. R. Hunt, O. M. Yaghi, *Nat. Chem.* **2010**, *2*, 235-238; b) S. Kandambeth, A. Mallick, B. Lukose, M. V. Mane, T. Heine, R. Banerjee, *J. Am. Chem. Soc.* **2012**, *134*, 19524-19527; c) H. Oh, S. B. Kalidindi, Y. Um, S. Bureekaew, R. Schmid, R. A. Fischer, M. Hirscher, *Angew. Chem.* **2013**, *125*, 13461-13464; *Angew. Chem., Int. Ed.* **2013**, *52*, 13219-13222; d) C. R. DeBlase, K. E. Silberstein, T. Truong, H. D. Abruña, W. R. Dichtel, *J. Am. Chem. Soc.* **2013**, *135*, 16821-16824; e) S. Chandra, T. Kundu, S. Kandambeth, R. BabaRao, M. Y. arathe, S. M. Kunjir, R. Banerjee, *J. Am. Chem. Soc.* **2014**, *136*, 6570-6573; f) Q. R. Fang, Z. B. Zhuang, S. Gu, R. B. Kaspar, J. Zheng, J. H. Wang, S. L. Qiu, Y. S. Yan, *Nat. Commun.* **2014**, *5*, 4503; g) T. Y. Zhou, S. Q. Xu, Q. Wen, Z. F. Pang, X. Zhao, *J. Am. Chem. Soc.* **2014**, *136*, 15885-15888; h) N. Huang, X. Chen, R. Krishna, D. L. Jiang, *Angew. Chem.* **2015**, *127*, 3029-3033; *Angew. Chem., Int. Ed.* **2015**, *54*, 2986-2990; i) S. Y. Ding, M. Dong, Y. W. Wang, Y. T. Chen, H. Z. Wang, C. Y. Su, W. Wang, *J. Am. Chem. Soc.* **2016**, *138*, 3031-3037; j) H. P. Ma, B. L. Liu, B. Li, L. M. Zhang, Y. G. Li, H. Q. Tan, H. Y. Zang, G. S. Zhu, *J. Am. Chem. Soc.* **2016**, *138*, 5897-5903; k) Q. Sun, B. Aguila, J. Perman, L. D. Earl, C. W. Abney, Y. Cheng, H. Wei, N. Nguyen, L. Wojtas, S. Q. Ma, *J. Am. Chem. Soc.* **2017**, *139*, 2786-2793; l) E. Q. Jin, M. Asada, Q. Xu, S. Dalapati, M. A. Addicoat, M. A. Brady, H. Xu, T. Nakamura, T. Heine, Q. H. Chen, D. L. Jiang, *Science* **2017**, *357*, 673-676; m) J. Roeser, D. Prill, M. J. Bojdys, P. Fayon, A. Trewin, A. N. Fitch, M. U. Schmidt, A. Thomas, *Nat. Chem.* **2017**, *9*, 977-982.
- [6] a) H. M. El-Kaderi, J. R. Hunt, J. L. Mendoza-Cortes, A. P. Côté, R. E. Taylor, M. O'Keeffe, O. M. Yaghi, *Science* **2007**, *316*, 268-272; b) F. J. Uribe-Romo, J. R. Hunt, H. Furukawa, C. Klöck, M. O'Keeffe, O. M. Yaghi, *J. Am. Chem. Soc.* **2009**, *131*, 4570-4571; c) D. Beaudoin, T. Maris, J. D. Wuest, *Nat. Chem.* **2013**, *5*, 830-834; d) G. Q. Lin, H. M. Ding, D. Q. Yuan, B. S. Wang, C. Wang, *J. Am. Chem. Soc.* **2016**, *138*, 3302-3305; e) L. A. Baldwin, J. W. Crowe, D. A. Pyles, P. L. McGrier, *J. Am. Chem. Soc.* **2016**, *138*, 15134-15137; f) Y. Z. Liu, Y. H. Ma, Y. B. Zhao, X. X. Sun, F. Gándara, H. Furukawa, Z. Liu, H. Y. Zhu, C. H. Zhu, K. Suenaga, P. Oleynikov, A. S. Alshammari, X. Zhang, O. Terasaki, O. M. Yaghi, *Science* **2016**, *351*, 365-369; g) Y. X. Ma, Z. J. Li, L. Wei, S. Y. Ding, Y. B. Zhang, W. Wang, *J. Am. Chem. Soc.* **2017**, *139*, 4995-4998.
- [7] a) Q. R. Fang, S. Gu, J. Zheng, Z. B. Zhuang, S. L. Qiu, Y. S. Yan, *Angew. Chem.* **2014**, *126*, 2922-2926; *Angew. Chem., Int. Ed.* **2014**, *53*, 2878-2882; b) Q. R. Fang, J. H. Wang, S. Gu, R. B. Kaspar, Z. B. Zhuang, J. Zheng, H. X. Guo, S. L. Qiu, Y. S. Yan, *J. Am. Chem. Soc.* **2015**, *137*, 8352-8355; c) H. Li, Q. Y. Pan, Y. C. Ma, X. Y. Guan, M. Xue, Q. R. Fang, Y. S. Yan, V. Valtchev, S. L. Qiu, *J. Am. Chem. Soc.* **2016**, *138*, 14783-14788; d) Z. L. Li, H. Li, X. Y. Guan, J. J. Tang, Y. Yusran, Z. Li, M. Xue, Q. R. Fang, Y. S. Yan, V. Valtchev, S. L. Qiu, *J. Am. Chem. Soc.* **2017**, DOI: 10.1021/jacs.7b11283.
- [8] a) D. N. Bunck, W. R. Dichtel, *Angew. Chem.* **2012**, *124*, 1921-1925; *Angew. Chem., Int. Ed.* **2012**, *51*, 1885-1889; b) D. N. Bunck, W. R. Dichtel, *Chem. Commun.* **2013**, *49*, 2457-2459; c) W. X. Gao, X. Y. Sun, H. L. Niu, X. J. Song, K. G. Li, H. C. Gao, W. X. Zhang, J. H. Yu, M. J. Jia, *Micro. Meso. Mater.* **2015**, *213*, 59-67.
- [9] a) V. Valtchev, G. Majano, S. Mintova, J. Perez-Ramirez, *Chem. Soc. Rev.* **2013**, *42*, 263-290; b) S. M. Cohen, *Chem. Rev.* **2011**, *112*, 970-1000.
- [10] C. Bonneau, O. Delgado-Friedrichs, M. O'Keeffe, O. M. Yaghi, *Acta Crystallogr.* **2004**, *A60*, 517-520.
- [11] Y. B. Zhang, J. Su, H. Furukawa, Y. F. Yun, F. Gandara, A. Duong, X. D. Zou, O. M. Yaghi, *J. Am. Chem. Soc.* **2013**, *135*, 16336-16339.
- [12] *Materials Studio ver. 7.0*; Accelrys Inc.; San Diego, CA.
- [13] a) Y. Sasaki, Y. Sugo, S. Suzuki, S. Tachimori, *Solvent Extr. Ion Exch.* **2001**, *19*, 91-103; b) N. Kumari, P. N. Pathak, D. R. Prabhu, V. K. Manchanda, *Sep. Sci. technol.* **2012**, *47*, 1492-1497.
- [14] a) U. Ehrstén, *Comprehensive Nuclear Materials* **2012**, *5*, 93-104; b) P. Carbol, D. H. Wegen, T. Wiss, P. Fors, *Comprehensive Nuclear Materials* **2012**, *5*, 389-420.
- [15] a) A. L. Myers, J. M. Prausnitz, *AIChE J.* **1965**, *1*, 121-127; b) S. Al-Asheh, F. Banat, R. Al-Omari, Z. Duvnjak, *Chemosphere* **2000**, *41*, 659-665; c) R. Krishna, B. Smit, S. Calero, *Chem. Soc. Rev.* **2002**, *31*, 185-194; d) S. Demir, N. K. Brune, J. F. V. Humbeck, J. A. Mason, T. V. Plakhova, S. Wang, G. Tian, S. G. Minasian, T. Tyliczszak, T. Yaita, T. Kobayashi, S. N. Kalmykov, H. Shiwaku, D. K. Shuh, J. R. Long, *Acc. Chem. Res.* **2016**, *49*, 253-265.
- [16] C. D. Wagner, W. M. Riggs, L. E. Davis, J. F. Moulder, G. E. Muilenberg, *Handbook of X-ray Photoelectron Spectroscopy*; Perkin Elmer: Eden Prairie, MN, 1979.

Covalent Organic Frameworks

Qiuyu Lu[†], Yunchao Ma[†], Hui Li, Xinyu Guan, Yusran Yusran, Ming Xue, Qianrong Fang*, Yushan Yan, Shilun Qiu and Valentin Valtchev*

_____ Page – Page

Postsynthetic Functionalization of Three-Dimensional Covalent Organic Framework for Selective Extraction of Lanthanide Ions



Here we report a general strategy for generating a 3D carboxyl-functionalized COF through postsynthetic modification of a hydroxyl COF, and for the first time explore the 3D carboxyl COF for selective extraction of lanthanide ions.